should help solve these problems.

ACKNOWLEDGMENTS

We acknowledge the kind help of Dr. Gouyette (Villejuif) for performing the FAB mass spectra.

REFERENCES

Bradbury, A. F., Finnie, M. D. A., & Smyth, D. G. (1982) *Nature (London) 298*, 686–688.
Bradford, M. M. (1976) *Anal. Biochem. 72*, 248–254.
Breslow, E. (1979) *Annu. Rev. Biochem. 48*, 251–274.
Camier, M., Alazard, R., Cohen, P., Pradelles, P., Morgat, J-L., & Fromageot, P. (1973) *Eur. J. Biochem. 32*, 207–214.
Chang, J. Y. (1983) *Methods Enzymol. 91*, 455–466.
Chang, J. Y., Knecht, R., & Braun, D. G. (1983) *Methods Enzymol. 91*, 41–48.
Clamagirand, Ch., Camier, M., Boussetta, H., Fahy, Ch., Morel, A., Nicolas, P., & Cohen, P. (1986) *Biochem. Biophys. Res. Commun. 134*, 1190–1196.
Clamagirand, Ch., Camier, M., Fahy, Ch., Clavreul, C., Creminon, Ch., & Cohen, P. (1987) *Biochem. Biophys. Res. Commun. 143*, 789–796.
Cohen, P. (1987) *Biochimie 69*, 87–89.
Cohen, P., Nicolas, P., & Camier, M. (1979) *Curr. Top. Cell. Regul. 15*, 263–318.
Cromlish, J. A., Seidah, N. G., & Chrêtien, M. (1986) *J. Biol. Chem. 261*, 10859–10870.
Eipper, B. A., Mains, R. E., & Glembotski, C. C. (1983) *Proc. Natl. Acad. Sci. U.S.A. 80*, 5144–5148.
Fuller, R., Brake, A., & Thorner, J. (1986) *Microbiology*, 273–278.
Gluschankof, P., & Cohen, P. (1987) *Neurochem. Res.* (in press).
Gluschankof, P., Morel, A., Gomez, S., Nicolas, P., Fahy, Ch., & Cohen, P. (1984) *Proc. Natl. Acad. Sci. U.S.A. 81*, 6662–6666.
Gluschankof, P., Morel, A., Benoit, R., & Cohen, P. (1985) *Biochem. Biophys. Res. Commun. 128*, 1051–1057.
Gomez, S., Di Bello, C., Than Hung, L., Genet, R., Morgat, J. L., Fromageot, P., & Cohen, P. (1984) *FEBS Lett. 167*, 160–164.
Ivell, R. (1986) *Curr. Top. Neuroendocrinol. 6*, 1–18.
Ivell, R., & Richter, D. (1984a) *Proc. Natl. Acad. Sci. U.S.A. 81*, 2006–2010.
Ivell, R., & Richter, D. (1984b) *EMBO J. 3*, 2351–2354.
Julius, D., Brake, A., Blair, L., Kunisawa, R., & Thorner, J. (1984) *Cell (Cambridge, Mass.) 37*, 1075–1089.
Kanmera, T., & Chaiken, I. M. (1985) *J. Biol. Chem. 260*, 10118–10124.
Land, H., Grez, M., Ruppert, S., Schmale, H., Rehbein, M., Richter, D., & Schütz, G. (1983) *Nature (London) 302*, 343–344.
Loh, Y. P., Parish, D. C., & Tuteja, R. (1985) *J. Biol. Chem. 260*, 7194–7205.
Masse, M. J. O., Desbois-Perichon, P., & Cohen, P. (1982) *Eur. J. Biochem. 127*, 609–617.
Merrifield, R. B. (1963) *J. Am. Chem. Soc. 85*, 2149–2154.
Mizuno, K., Kojima, M., & Matsuo, H. (1985) *Biochem. Biophys. Res. Commun. 128*, 884–891.
Nicolas, P., Delfour, A., Boussetta, H., Morel, A., Rholam, M., & Cohen, P. (1986) *Biochem. Biophys. Res. Commun. 140*, 565–573.
Parish, D. C., Tuteja, R., Altstein, M., Gainer, H., & Loh, Y. P. (1986) *J. Biol. Chem. 261*, 14392–14397.
Rholam, M., Nicolas, P., & Cohen, P. (1986) *Fed. Eur. Biochem. Soc. Lett. 207*, 1–6.

Conformation of the ATP Binding Peptide in Actin Revealed by Proton NMR Spectroscopy†

Julian A. Barden

Muscle Research Unit, Department of Anatomy, The University of Sydney, Sydney, NSW 2006, Australia

Received December 10, 1986; Revised Manuscript Received April 8, 1987

ABSTRACT: The actin peptide 106–124 exists in a completely conserved region of the sequence and binds strongly to both ATP and tripolyphosphate. Binding particularly affects residues 116 and 118 and generally affects the two segments 115–118 and 121–124 [Barden, J. A., & Kemp, B. E. (1987) *Biochemistry 26*, 1471–1478]. One-dimensional nuclear Overhauser enhancement difference spectroscopy was used to detect molecular interactions between both adjacent and nonadjacent residues. The N-terminal segment 106–112 was found to be largely extended. A sharp bend was detected between Pro-112 and Lys-113. The triphosphate moiety binds to the strongly hydrophilic central segment of the peptide. Evidence was obtained for a reverse turn involving residues 121–124. Amide proton temperature coefficients and coupling constants provide evidence for a type I β-turn. A model of the ATP binding site is proposed together with its relationship to other parts of the actin structure and to the phalloidin binding site.

Actin filaments are assembled, disassembled, and reorganized in cells. These processes provide a basis for the several behavioral, contractile, and structural events occurring in the cells (Korn, 1982).

The tertiary structure of actin has been determined at a resolution of 0.45 nm (Kabsch et al., 1985). Although this resolution is not yet sufficient to enable the backbone of the peptide chain to be followed, the electron density map reveals that there are two major domains. These are separated by a pronounced cleft, at the base of which is the triphosphate moiety of the bound ATP. Actin monomers denature in the absence of the bound nucleotide (Asakura, 1961; Waechter & Engel, 1977). Thus, the binding of ATP appears to be needed to stabilize the structure of the cleft region. Moreover, the nucleotide is dephosphorylated following the incorporation

† This work has been supported by a grant from the National Health and Medical Research Council of Australia.

0006-2960/87/0426-6023$01.50/0

of the ATP–actin monomer into the actin filaments. ATP hydrolysis appears to be uncoupled from monomer addition; rather, it occurs as a result of an enhancement in the ATPase activity of the subunits within the actin filament (Pardee & Spudich, 1982; Carlier et al., 1984; Pollard & Weeds, 1984). The ADP is essentially unable to be exchanged in F-actin other than at the filament ends and thus appears to be sterically blocked by the actin–actin interaction. Consequently, the nucleotide may also have a role in treadmilling, particularly in nonmuscle contractile systems (Wegner, 1976; Kirschner, 1980; Neuhaus et al., 1983; Wanger et al., 1985).

The nucleotide and phalloidin binding sites are overlapped, with phalloidin sterically blocking the exchange of the nucleotide (Barden et al., 1987). Arg-116 and Lys-118 appear to be the most important residues responsible for binding ATP (Barden et al., 1987; Barden & Kemp, 1987). These residues are adjacent to Glu-117 and Met-119 which can be cross-linked to phalloidin (Vandekerckhove et al., 1985). Another region of the actin sequence close to the phalloidin binding site is Met-355 (Vandekerckhove et al., 1985), which is next to Trp-356, a residue able to be cross-linked to 8-azido-ATP (Hegyi et al., 1986).

Both ATP and tripolyphosphate bind to the actin peptide 106–124 with high affinity (Barden & Kemp, 1987), and thus, the isolated peptide can be expected to provide a good model for the ATP binding site in actin. In this paper, an analysis of the peptide structure is made by using the results of measurements of nuclear Overhauser effects between adjacent and nonadjacent side chains, the alteration in chemical shift and size of the $^3J_{NHCH}$ coupling constants when the peptide is unfolded in urea, and the torsion angles, ϕ, determined from the Karplus equations. A Corey–Pauling–Koltun (CPK) space-filling model of the peptide is presented showing the likely relationship between the peptide and ATP.

Materials and Methods

Synthesis and Purification of Actin Peptide 106–124. The actin peptide 106–124 was synthesized by using the solid-phase synthesis procedure as described earlier (Barden & Kemp, 1987).

Proton NMR Spectroscopy. Proton resonance assignments of the peptide in D_2O and H_2O at pH 5 were determined in an earlier paper (Barden & Kemp, 1987). The peptide was lyophilized in 99.8% D_2O and then in 100% D_2O. Those measurements which included the NH resonances were obtained by lyophilizing the peptide from pure H_2O. Sample pH was adjusted with NaOD or DCl and measured with an Activon BJ51130 thin-stem NMR microelectrode and a Radiometer pHM-64 meter. Values reported are meter readings uncorrected for the deuterium isotope effect. the concentration of the synthetic actin peptide 106–124 had to be maintained below 3.0 mM to ensure complete solubility. Evidence of line broadening and amide proton chemical shift changes was obtained at peptide concentrations of 4.0 mM and above in the pH range 2.5–6.5. Solubility was progressively reduced outside this pH range. All samples were scanned in 5-mm precision tubes.

NMR spectra were recorded at 298 K at 400 MHz in the Fourier transform mode with quadrature detection using a Varian XL-400 spectrometer. The one-dimensional (1-D) spectra of samples in D_2O were collected by using a 90° radio-frequency pulse of 13 μs. A spectral width of 4 kHz was employed with a preacquisition delay of 2.0 s. The acquisition time was 2.0 s, and generally 1024 scans were collected.

The amide and some side chain resonance assignments were redetermined in samples containing urea up to 8 M using a 1-D spin decoupling procedure. The low peptide concentrations used precluded the use of 2-D techniques for the assignment of NH resonances. Following assignment of the αCH resonances in 8 M urea, all the NH resonances were assigned by using a two-level 1-D spin decoupling procedure. The solvent resonance was irradiated with homodecoupling continuously throughout a 2.0-s preacquisition and a 1.0-s acquisition period while a low level decoupling pulse was applied during the acquisition period to a selected αCH resonance. The coupled NH resonance was then observed to collapse to a singlet.

1-D NOE difference spectra were obtained with a preacquisition delay of 2.0 s and a saturation time of 4.0 s by the method of Jones et al. (1978). A total of 1024 scans were collected with alternate blocks of 32 on-resonance and off-resonance pulses each preceded by 4 dummy scans. The residual solvent resonance was irradiated simultaneously using a two-level pulse scheme. All chemical shifts were referenced to internal (trimethylsilyl)propanesulfonic acid (TSS).

Results

NMR of the ATP Binding Actin Peptide. The ATP binding site in actin resides within the segment 106–124 which has the sequence Thr-Glu-Ala-Pro-Leu-Asn-Pro-Lys-Ala-Asn-Arg-Glu-Lys-Met-Thr-Gln-Ile-Met-Phe (Barden & Kemp, 1987). A 1-D composite spectrum of a 3.0 mM solution of the peptide obtained in D_2O and in H_2O at 298 K and pH 3.0 is shown in Figure 1. The amide resonances (7–9 ppm) were detected in H_2O with the remainder detected in D_2O. Several of the assigned resonances reveal the presence of structured segments in the peptide (Barden & Kemp, 1987). These include a 0.24 ppm downfield shift, relative to the position expected in small unstructured peptides (Bundi & Wüthrich, 1979), in the αCH of Ala-108 due to its close proximity to the Pro-109 ring (Grathwohl & Wüthrich, 1976a,b; Schulz & Schirmer, 1979). Identical results have been observed in other Ala-Pro sequences in the trans configuration (Bhandari et al., 1986). A similar shift is observed in the αCH of Asn-111 for the same apparent reason, and there is a smaller upfield ring current shift in the ϵCH_3 singlet resonance of Met-123 due to the proximity of the aromatic ring of Phe-124.

The binding of tripolyphosphate was observed to affect segments 115–118 and 121–124 (Barden & Kemp, 1987), indicating the likely presence of a reverse turn between them. Thus, the peptide was studied under denaturing conditions in 8 M urea to compare the structures, particularly as evidenced by the changes in the chemical shifts of the amide resonances. While most of the side chain resonances are affected only to a small extent by the presence of 8 M urea, there are significant exceptions. Figure 2 shows a comparison between the spectra in the absence and presence of 8 M urea in the regions 1.6–1.9, 2.9–3.3, and 8.2–8.6 ppm. These changes primarily involve the downfield shift of the δCH_2 resonances of Lys-118 from 1.663 to 1.746 ppm, i.e., close to the βCH_2 resonances of Ile-122, and the downfield shift of the ϵCH_2 resonances of Lys-118 from 3.003 to 3.071 ppm. In the amide region, there is an upfield shift in the Gln-121 NH resonance from 8.823 to 8.516 ppm, a downfield shift in the Ala-108 NH from 8.487 to 8.211 ppm, an upfield shift in the Leu-110 NH from 8.114 to 8.432 ppm, and an upfield shift of the Asn-111 NH from 8.487 to 8.878 ppm as the peptide is largely unfolded in the urea.

Amide Proton Resonance Assignments. A complete assignment of the amide resonances is presented in Table I both in the absence and in the presence of 8 M urea at pH 5.0 and 298 K together with the values reported in the unstructured tetrapeptides Gly-Gly-X-Ala (Bundi & Wüthrich, 1979). The

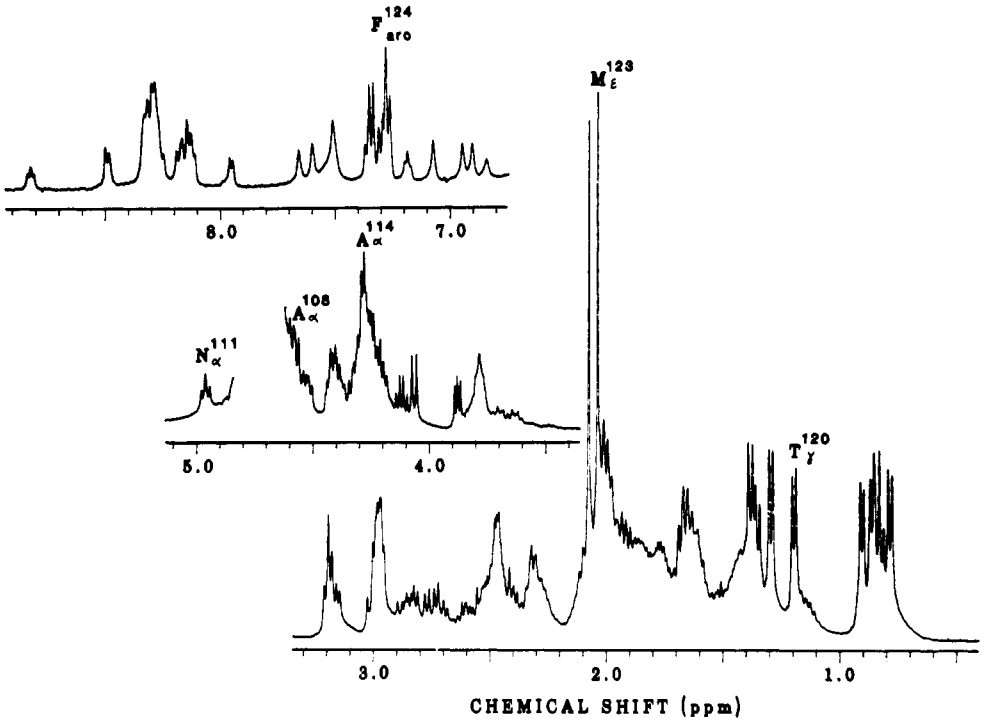

FIGURE 1: Composite proton NMR spectrum at 400 MHz of the actin peptide 106–124, constituting the ATP binding site. The sample was 3.0 mM in either D_2O or H_2O (spectral region 7–9 ppm) at pH 3.0 and 298 K. Several resonances have been identified on the figure. The single-letter codes of the amino acid residues are A (Ala), F (Phe), M (Met), N (Asn), Q (Gln), and T (Thr).

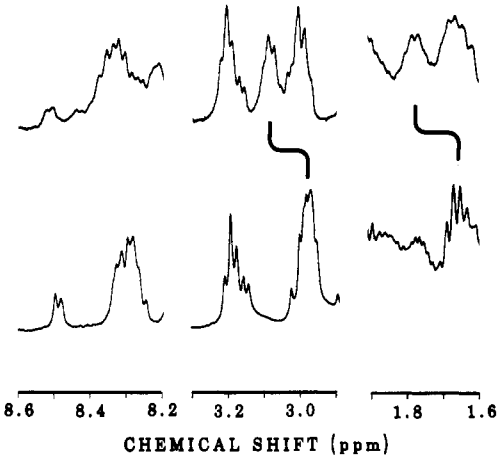

FIGURE 2: Effects of unfolding the peptide in 8 M urea on the chemical shift of the proton resonances are illustrated in three regions of the spectrum: 1.6–1.9, 2.9–3.3, and 8.2–8.6 ppm. The two upfield regions show changes in the environment of Lys-118. The δCH_2 moves from 1.663 to 1.746 ppm and the ϵCH_2 from 3.003 to 3.071 ppm. The amide region shows substantial changes in the environments of Ala-108, Leu-110, Asn-111, and Gln-121 as summarized in Table I.

Table I: Chemical Shifts of the Amide Backbone Proton Resonances (Referenced to Internal TSS) in the Actin Peptide 106–124 at 298 K, 3.0 mM, and pH 5.0 in the Absence and Presence of 8 M Deuteriated Urea in 80% H_2O and 20% D_2O[a]

	chemical shift (ppm)		
residue	no urea	8 M urea	tetrapeptides
Glu-107	8.310	8.360	8.368
Ala-108	8.487	8.211	8.249
Leu-110	8.114	8.432	8.423
Asn-111	8.487	8.878	8.747
Lys-113	8.278	8.332	8.408
Ala-114	7.949	8.063	8.249
Asn-115	8.809	8.910	8.747
Arg-116	8.270	8.280	8.274
Glu-117	8.121	8.230	8.368
Lys-118	8.278	8.332	8.408
Met-119	8.317	8.367	8.418
Thr-120	8.276	8.332	8.236
Gln-121	8.823	8.516	8.411
Ile-122	8.121	8.218	8.195
Met-123	8.317	8.367	8.418
Phe-124	8.176	8.247	8.228

[a] Amide proton chemical shifts in unstructured tetrapeptides [from Bundi and Wüthrich (1979)] are included for comparison and are largely unaffected by urea.

major shifts in the amide resonances which accompany the addition of urea include those from Ala-108, Leu-110, Asn-111, Ala-114, Asn-115, Glu-117, Gln-121, Ile-122, and Phe-124. The remaining amide resonances are affected to lesser extents, and in general, the chemical shifts observed in 8 M urea are close to those expected from an unordered structure (Bundi & Wüthrich, 1979).

Coupling Constants. The $^3J_{NHCH}$ coupling constants derived from the fine structure of the amide proton resonances are listed in Table II. The effect of urea on the unfolding of the peptide is evidenced by the increased values of the coupling constants as shown in the fourth column. Small changes in temperature (5 K around 298 K) were used to differentiate the different amides that were partially overlapped. However, the two Met amides and the two Lys amides were each fully overlapped under all conditions tested. The overlapped amide resonances of Asn-111 and Ala-108 were readily separated with small temperature changes as was the case with the Thr-120 amide which was overlapped by the pair of Lys resonances. The overlapped Glu-117 and Ile-122 amides at 8.121 ppm similarly were separated with small temperature changes. The measured values of $^3J_{NHCH}$ in the absence of urea and the Karplus relations were used to calculate the torsional angles, ϕ. The parameters employed in the calculations are derived from data for the ferrichromes (De Marco et al., 1978) by using the equation:

$$^3J_{NHCH} = 5.41 \cos^2(\phi - 60°) - 1.27 \cos(\phi - 60°) + 2.17$$

Although the solid-state and solution structures of these rigid

Table II: $^3J_{NHCH}$ Coupling Constants and Torsional Angles (ϕ) at 298 K and pH 5.0 in the Absence of Urea[a]

residue	no urea		8 M urea,	% increase,
	J (Hz)	ϕ (deg)	J (Hz)	0–8 M urea
Glu-107	7.6	−147, −93	7.6	0
Ala-108	6.0	−166, −77, 45, 75	6.8	13
Leu-110	5.6	−167, −74, 37, 84	6.8	25
Asn-111	6.0	−163, −77, 45, 75	7.6	27
Lys-113	5.2	−172, −70, 30, 92	6.6	27
Ala-114	5.2	−172, −70, 30, 92	6.8	31
Asn-115	5.2	−172, −70, 30, 92	7.5	25
Arg-116	6.0	−163, −77, 45, 75	6.8	13
Glu-117	7.2	−151, −89	7.6	6
Lys-118	5.2	−172, −70, 30, 92	6.6	27
Met-119	6.8	−156, −85	7.6	18
Thr-120	6.0	−163, −77, 45, 75		
Gln-121	5.2	−172, −70, 30, 92	7.6	46
Ile-122	6.6	−158, −82	6.8	3
Met-123	6.8	−156, −85	7.6	12
Phe-124	6.4	−160, −80	8.4	31

[a] Values of $^3J_{NHCH}$ measured in 8 M urea and the percent increase in J between 0 and 8 M urea are also presented as a measure of the effect of urea-induced unfolding.

Table III: Temperature Coefficients of the Amide Proton Resonances in the Absence and Presence of 8 M Urea at pH 5.0

residue	$-d\delta/dT$ (ppb/K) at [urea] (M) of		% increase, 0–8 M urea
	0	8	
Glu-107	7.0	7.5	7
Ala-108	8.7	8.7	0
Leu-110	7.4	7.6	3
Asn-111	8.3	8.7	5
Lys-113	7.3	8.6	18
Ala-114	5.4	6.4	19
Asn-115	6.5	8.8	34
Arg-116	5.7	8.4	47
Glu-117	5.8	7.6	31
Lys-118	5.4	8.6	59
Met-119	6.6	7.2	9
Thr-120	6.4	8.4	31
Gln-121	6.5	8.7	34
Ile-122	6.0	7.6	27
Met-123	5.2	7.2	38
Phe-124	5.9	8.7	47

peptides are believed to be the same (De Marco et al., 1978), the torsional angles for the ATP binding peptide are likely to be weighted averages over more than one conformation.

Amide Proton Temperature Coefficients. Variations in the chemical shifts of the NH amide proton resonances were measured over the temperature range 293–328 K. A linear least-squares regression analysis resulted in the values of $-d\delta/dT$ (ppb/K) listed in Table III both in the absence and in the presence of 8 M urea. Since all the chemical shift vs. temperature relations were linear, gaps in the curves were left for those temperatures where the amide resonances were overlapped. Nevertheless, a minimum of eight points were available for each amide temperature coefficient determination. The chemical shifts of the αCH protons were essentially invariant with changes in temperature (Higashima et al., 1979). The N-terminal residues display values for the coefficients which are higher than those displayed by the C-terminal residues from Lys-113 to Phe-124. However, in 8 M urea, the temperature coefficients of these C-terminal residues increase disproportionately with respect to the N-terminal residues. The percentage increase for each amide proton is listed in Table III. The resonances displaying the lowest temperature coefficients in water experience the largest increases in the presence of urea. Such a result would be expected to accompany the unfolding of a structured C-terminal region.

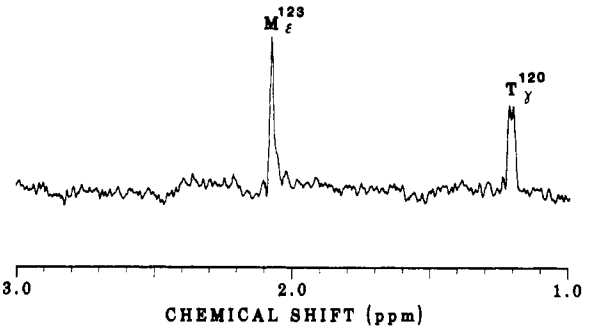

FIGURE 3: NOE difference spectrum obtained by selectively irradiating the aromatic Phe resonance in Figure 1. Interresidue NOEs are detected in the Thr-120 γCH_3 and the Met-123 ϵCH_3.

Nuclear Overhauser Effects. Nuclear Overhauser effects were measured between protons both from adjacent and from non adjacent residues in the sequence. The existence of a medium to strong NOE between protons on nonadjacent residues indicates that they are within an average range of about 0.3 nm for mutual dipolar relaxation to occur. These measurements are consequently a major indicator of the presence of a peptide conformation with high statistical weight.

All proton resonance assignments were determined unambiguously by using two-quantum-filtered COSY and NOE spectra. The NOEs were detected by using 1-D experiments since the peptide concentration had to be maintained at or below 3 mM to avoid aggregation (Barden & Kemp, 1987). Aside from the expected intraresidue effects, a number of interresidue NOE effects were observed in the N-terminal region of the peptide. However, no NOE effects in this region were observed between nonadjacent residues. NOEs were measured between the αCH of Ala-108 and the δCH_2 resonances of Pro-109 as expected for an Ala–Pro bond which is clearly in the trans configuration as described above. The β- and γ-protons of Pro-109 were found to interact with the δCH_3 protons on the adjacent Leu-110, and the αCH of Asn-111 was found to interact with the δ-protons of Pro-112. This latter NOE was also expected after a large downfield shift in the αCH resonance of Asn-111 was observed (Barden & Kemp, 1987) and also verifies that the Asn-Pro bond is in the trans configuration (Bhandari et al., 1986). Another NOE was measured between the δCH_2 protons of Pro-112 and the βCH_2 protons on the adjacent Lys-113. No other NOE effects were detected between side chains of residues in the polar segment consisting of Lys-113 to Lys-118 inclusive.

In the C-terminal segment of the peptide, several NOE effects were measured which involved interactions between nonadjacent side chains. Interresidue NOE effects were measured between the γCH_3 protons of Thr-120 and the γ- and ϵ-protons of the adjacent Met-119 as well as the aromatic ring of the nonadjacent Phe-124. Furthermore, NOEs were measured between the aromatic ring of Phe-124 and the ϵCH_3 protons of Met-123. These provide strong evidence that the C-terminal residues occupy a weighted conformation in the form of a reverse turn. Figure 3 shows the NOE difference spectrum obtained by irradiating the aromatic resonances of Phe-124.

Effect of Gd Binding. Gadolinium is a paramagnetic lanthanide ion which acts to broaden the resonances of nearby protons. A stock solution of $GdCl_3$ was standardized (Barden & dos Remedios, 1978), adjusted to 75 mM, and titrated into a 2.5 mM solution of the peptide at pH 4.0. The pH of the $GdCl_3$ stock in D_2O was also maintained at 4.0. The Gd ions bind to the carboxyl side chains of Glu-107 and Glu-117.

Table IV: Degree of Gd-Induced Broadening of Resonances of Nearby Protons[a]

resonance	intensity loss (%)	resonance	intensity loss (%)
Thr-106 α	12	Arg-116 γ	13
Thr-106 β	19	Glu-117 γ	100
Glu-107 γ	100	Lys-118 α	20
Ala-108 β	11	Lys-118 γ	16
Pro-109 δ	6	Met-119 ϵ	22
Arg-116 α	18		

[a] The Gd:peptide ratio was 1:10, just sufficient to completely broaden the γCH_2 resonances of the Glu residues.

Several resonances are partially broadened as a result of the binding. Apart from the γCH_2 resonances of Glu-107 and Glu-117 at 2.427 ppm, the resonances most affected include the αCH and βCH of Thr-106 at 3.883 and 4.135 ppm, respectively, the βCH_3 of Ala-108 at 1.373 ppm, the δCH_2 of Pro-109 at 3.803 and 3.719 ppm, the αCH and γCH_2 of Arg-116 at 4.375 and 1.625 ppm, respectively, the αCH and γCH_2 of Lys-118 at 4.302, 1.460, and 1.403 ppm, respectively, and the ϵCH_3 of Met-119 at 2.097 ppm. The degree to which these resonances were broadened, as measured by the reduction in resonance intensity in the presence of 0.25 mM $GdCl_3$, is shown in Table IV.

Discussion

Binding of ATP to the peptide 106–124 occurs via an electrostatic interaction between the positively charged side chains of Arg-116 and Lys-118 and the negatively charged terminal phosphates of the triphosphate side chain. Moreover, residues 121–124 appear to be affected by the binding of tripolyphosphate (Barden & Kemp, 1987).

The chemical shifts of the amide proton resonances were measured. These were compared to the chemical shifts of these same protons in small unstructured peptides and to those measured following the unfolding of the peptide in 8 M urea (Table I). The comparison revealed that several of the residues are in structured environments. The amides of Ala-108, Leu-110, Asn-111, and Gln-121 display chemical shifts with the largest divergence from the random coil positions. However, in the presence of 8 M urea, these amide resonances all move close to the values expected in a random coil. Other residues also exhibit amide proton chemical shifts that are suggestive of an ordered environment. These include Ala-114, Asn-115, Glu-117, Ile-122, and Phe-124.

Measurement of the temperature coefficients ($-d\delta/dT$) for the amide protons reveals that the N-terminal residues exhibit generally higher values than the C-terminal residues and are thus less likely to be involved in an averaged ordered conformation. The presence of the two Pro residues (Pro-109 and -112) which form Ala-Pro and Asn-Pro bonds in the trans configuration produces chemical environments leading to large shifts in the amide proton resonances of Ala-108, Leu-110, and Asn-111. As the data in Table II show, unfolding of the peptide in 8 M urea causes a disproportionate increase in the temperature coefficients of residues 113–124. In 8 M urea, the coefficients of the resonances in the N- and C-terminal segments are all similar. The largest increases observed when the peptide is unfolded in 8 M urea are in Asn-115, Arg-116, Lys-118, Gln-121, Met-123, and Phe-124. These are the same residues that are most affected by the binding of tripolyphosphate (Barden & Kemp, 1987). The temperature coefficients of the amide proton chemical shifts are useful indicators of the relative accessibility of these protons to the solvent (Kopple et al., 1963). The relatively lower values displayed by the above residues, and which do not pertain in urea, indicate that they occupy an environment which, on average, is more protected from solvent than the N-terminal residues. The urea acts to break the structures which may tend to form hydrogen bonds.

The $^3J_{NHCH}$ coupling constants reveal similar increases when the peptide is unfolded in urea (Table II). The largest increases are recorded for residues Gln-121, Phe-124, Lys-118, and the segment Leu-110 to Asn-115. These results provide further support for the conclusion that, on average, much of the peptide occupies a structured conformation.

The NOEs observed between Phe-124 and the nonadjacent residue Thr-120 demonstrate that the peptide contains a nonextended structure in the C-terminal region. It is very likely that many NOEs remained undetected at 400 MHz and so many of the short interproton interactions have not been determined. Even so, those that have been detected provide substantial constraints on the range of permissible structures.

NOEs detected between the six C-terminal residues, and between Phe-124 and Thr-120 in particular, indicate the presence of a reverse turn. The 0.4 ppm downfield shift in the resonance of the Gln-121 amide proton is in full accordance with such a structure which would involve a hydrogen bond formed between the CO of Gln-121 and the NH of Phe-124. The Phe ring must interact closely with the Gln-121 NH. Such a close average proximity would explain the large downfield ring current shift in the Gln-121 NH (Johnson & Bovey, 1958; Jardetsky & Roberts, 1981). The type of β-turn formed can be deduced from the determination of the torsional angles, ϕ, calculated from the Karplus equation as described above. Only two torsional angles can be calculated for each of the residues Ile-122 and Met-123 (Table II). The single sterically possible pair is $-82°$, $-85°$, i.e., close to the theoretical values applying for a type I β-turn ($-60°$, $-90°$). The low value of the temperature coefficient of the amide proton resonance of Met-123, especially when compared to the value in the unfolded state in urea, provides an indication that this proton is less accessible to the solvent than most of the other amides. This adds further support to the conclusion that the structure is a type I β-turn. The temperature coefficient of the Phe-124 NH is 47% higher in the presence of 8 M urea where the peptide is unfolded. This value in H_2O is perhaps not as low as it would be in the presence of additional C-terminal residues which might act to stabilize the β-turn. Consequently, the value does not provide unequivocal evidence of a H-bond formation with the CO of Gln-121. Nevertheless, the interresidue NOEs lend very strong support for the view that in the intact protein or a larger polypeptide enclosing this sequence, a H-bond exists between these two residues.

The N-terminal seven residues appear from the NOE data to take on an extended conformation. The average proximity of the αCH of Ala-108 is close to the ring of Pro-109 which demonstrates that this is a trans peptide bond and thus is extended. In a similar fashion, the average proximity of the αCH of Asn-111 is close to the ring of Pro-112 and thus is also extended. An NOE also was detected between the δCH_3 protons of Leu-110 and the adjacent β-protons and γCH_2 protons of Pro-109. These interactions likewise are consistent with the Pro-Leu peptide bond being maintained in an extended conformation.

A sharp bend between Pro-112 and Lys-113 is in evidence with an NOE between the δCH_2 of Pro-112 and the βCH_2 of Lys-113. On average, the backbone appears to undergo a right-angle bend with the axis running along the Lys side chain being parallel to the plane of the Pro ring. The Lys-113–

Ala-114 peptide bond is exposed to solvent in G-actin since it can be cleaved by thrombin (Muszbek & Laki, 1974). Moreover, Lys-113 can be modified in G-actin but not in F-actin (Lu & Szilagyi, 1981; Hitchcock-de Gregori et al., 1982) and thus appears to reside at an actin–actin interface (Hambly et al., 1986). The Pro–Lys bend may indicate either that residues 106–112 are located internally within the tertiary structure of actin or that Lys-113 is located on an exposed edge.

No NOEs were detected between residues in the segment 113–119; however, two observations about this region are pertinent. First, Arg-116 and Lys-118 interact with the terminal phosphates of the bound ATP (Barden et al., 1987; Barden & Kemp, 1987), and second, affinity labeling derivatives of phalloidin can be cross-linked to Glu-117 and Met-119. These four residues therefore must be surface accessible. Since the phosphates of the bound ATP are situated in the base of the cleft between the two domains in actin (Kabsch et al., 1985), the segment 116–119 must be situated at the base of the cleft with the side chains situated in the solvent. For the triphosphate moiety to bind to the side chains of Arg-116 and Lys-118 requires these two side chains to be oriented approximately parallel with one another. For phalloidin to bind simultaneously to the side chains of Glu-117 and Met-119 similarly implies that these two side chains must be oriented approximately parallel with one another. The absence of NOEs between any of these four side chains and the requirement that all must be surface accessible indicate that alternate side chains are probably oriented no closer than about right angles to each other. In relation to orthogonal axes, the axis through the side chains of Arg-116 and Lys-118 is oriented along $+X$ while the axis through the side chains of Glu-117 and Met-119 is oriented along $+Y$ and the axis through the peptide backbone is oriented along $-Z$. These orientations of course are meant only as approximations. The compact structure of the C-terminal six residues is thus adjacent to Lys-118. Table IV reveals that the αCH and γCH_2 resonances of both Arg-116 and Lys-118 appear to be almost equidistant from the γCH_2 of Glu-107. The ϵCH_3 of Met-119 appears to be slightly closer to Glu-117 than either the αCH of Arg-116 or Lys-118.

The peptide appears to be divided into three distinct segments. The first consists of residues 106–112, the second consists of residues 113–118, and the third consists of residues 119–124. The average hydrophobicity of residues in the three segments was calculated to be −2.0, 7.8, and −5.0 kJ/mol, respectively (Nozaki & Tanford, 1971; Chothia, 1974; Levitt, 1976). Thus, the first segment is relatively hydrophobic and as discussed above may largely be buried within the actin structure. The third segment is extremely hydrophobic, with the ring of the Phe projecting back over the backbone of the residues making up the type I β-turn. Such a segment can largely be expected to be buried within the tertiary structure. The middle segment, on the other hand, is extremely hydrophilic, as expected from surface-accessible ionic binding sites.

A CPK space-filling model of the peptide sequence was assembled, and the accumulated NMR data were used to reconstruct the likely solution conformation (Figure 4). The manner in which the Phe-124 side chain projects back over the β-turn to interact with the other residues is clear from the model. This makes the C-terminus quite hydrophobic and compact. The N-terminal segment 106–112 is extended. The large-angle bend in the peptide chain between Pro-112 and Lys-113 (see arrow) leaves the Lys side chain projecting well out into the solvent. In Figure 5A, a different view of the

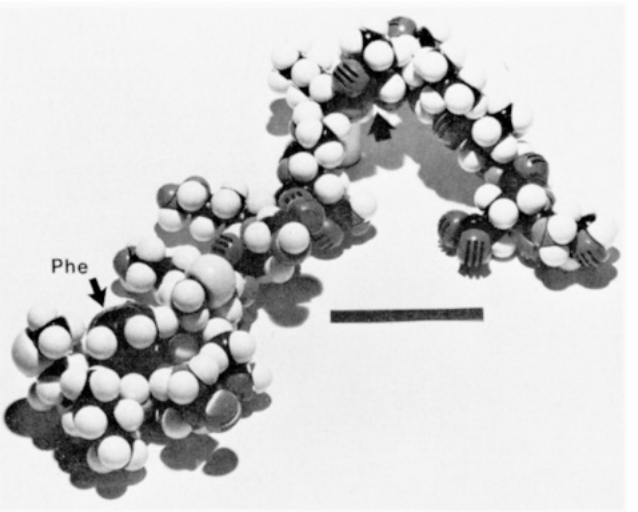

FIGURE 4: CPK model of the peptide 106–124 consistent with the NMR data. The model displays a conformation of high statistical weight, incorporating the known relationship between the ATP and phalloidin binding sites. The bar scale is 1.0 nm in length. The side chain of Phe-124 (labeled) can be seen projecting back over the type I β-turn, and the sharp bend between Pro-112 and Lys-113 is clearly visible (arrow).

segment 113–124 is shown. The distance between the side chain of Phe-124 from the side chain of Lys-113 is 3 nm. In Figure 5B, the ATP moiety has been added to the peptide in the only conformation which appears likely. The base of the ATP is in the probable syn conformation (Tanswell et al., 1975), and thus, Trp-356 is probably located over the top of Met-123 in the tertiary structure, close to the 8-position on the adenosine (Hegyi et al., 1986). In this way, the adjacent Met-355 is probably closer to the top of Gln-121 so that it can be cross-linked to phalloidin (Vanderkerckhove et al., 1985).

The γ-phosphate is complexed to Arg-116 and the β-phosphate to Lys-118. The α-phosphate is probably not strongly involved in binding to actin (Cozzone et al., 1974; Brauer & Sykes, 1981), but to the extent that it is involved, it will bind to Lys-118. The adenosine moiety (shown in the syn configuration) ring stacks with Phe-124. While the adenosine normally interacts with actin (Mihashi & Wahl, 1975), it can be mobilized (Barden et al., 1980; Curmi et al., 1982). A Trp residue is then partially exposed. This is presumably Trp-356 which is adjacent to the adenosine (Hegyi et al., 1986). A Phe may also be exposed (Phe-124), but the loss of hypochromicity due to the mobilization of the adenosine masks the UV difference effects at 250–265 nm of Phe exposure (Curmi et al., 1982). The 2-position of adenosine can be cross-linked to Tyr-306 (Kuwayami & Yount, 1986). The model clearly shows that such a positioning of Tyr-306 is possible below the side chain of Lys-118 and the α- and β-phosphates.

Had the ATP been placed in the opposite orientation, the adenosine would have interfered directly with the side chain of Lys-113, which is on an exposed portion of the surface at an actin–actin interaction site (Hambly et al., 1986) and not in the cleft as shown by Kabsch et al. (1985). It is therefore expected that the model of the ATP binding site presented in Figure 5 is close to the structure of the site in native actin.

The spatial relationship of the nucleotide binding site in actin to other labeled sites in the monomer (Miki & Wahl, 1984; dos Remedios & Cooke, 1984; Barden & Miki, 1986; Miki et al., 1986), in combination with the NMR results presented in this paper, will aid our understanding of the actin structure. This will prove especially true when the crystal structure of actin becomes more refined. Moreover, the study of the

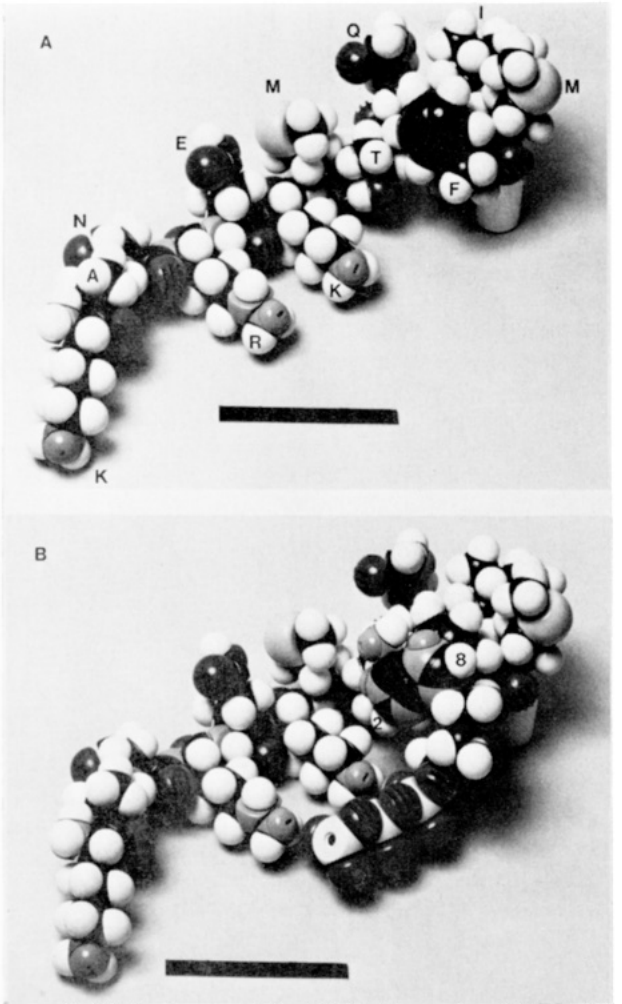

FIGURE 5: (A) A close-up of the ATP binding region of the peptide including residues 113–124. The residues are labeled on the figure by using the single-letter codes for the amino acids: K, Lys; A, Ala; N, Asn; R, Arg; E, Glu; M, Met; T, Thr; Q, Gln; I, Ile; and F, Phe, sequentially. Note how the ϵCH_3 of Met-119 interacts with the γCH_3 of Thr-120 which in turn is close to the aromatic ring of Phe-124. The side chains of Arg-116 and Lys-118 are at approximately a right angle to the side chains of Glu-117 and Met-119. These four residues as well as Lys-113 are all surface accessible and are located in a highly hydrophilic segment of the peptide. (B) The same view as in (A) but with ATP added in the likely syn configuration. The adenosine ring stacks with the Phe side chain, and the two terminal phosphates bind to the side chains of Arg-116 and Lys-118. Note that the 8-position of adenosine (labeled) projects up toward the top of Met-123 while the 2-position projects below Lys-118 and the α- and β-phosphates. The bar scale is 1.0 nm in length.

structure of the ATP binding site in actin should prove of more general interest to the study of the homologous nucleotide sites in other proteins (Walker et al., 1982; Argos & Leberman, 1985). Furthermore, knowledge of the structure of the ATP site in actin will assist in our understanding of the function of the actin-bound nucleotide in the contractile process.

ACKNOWLEDGMENTS

I thank Drs. G. L. Mendz and C. G. dos Remedios for helpful discussions.

Registry No. ATP, 56-65-5; actin segment 106–124, 106436-19-5.

REFERENCES

Argos, P., & Leberman, R. (1985) *Eur. J. Biochem. 152*, 651–656.
Asakura, S. (1961) *Arch. Biochem. Biophys. 92*, 140–149.
Barden, J. A., & dos Remedios, C. G. (1978) *Biochim. Biophys. Acta* 537, 417–427.
Barden, J. A., & Miki, M. (1986) *Biochem. Int. 12*, 321–329.
Barden, J. A., & Kemp, B. E. (1987) *Biochemistry 26*, 1471–1478.
Barden, J. A., Cooke, R., Wright, P. E., & dos Remedios, C. G. (1980) *Biochemistry 19*, 5912–5916.
Barden, J. A., Miki, M., Hambly, B. D., & dos Remedios, C. G. (1987) *Eur. J. Biochem. 162*, 583–588.
Bhandari, D. G., Levine, B. A., Trayer, I. P., & Yeadon, M. E. (1986) *Eur. J. Biochem. 160*, 349–356.
Brauer, M., & Sykes, B. D. (1981) *Biochemistry 20*, 6767–6775.
Bundi, A., & Wüthrich, K. (1979) *Biopolymers 18*, 285–297.
Carlier, M.-F., Pantaloni, D., & Korn, E. D. (1984) *J. Biol. Chem. 259*, 9983–9986.
Chothia, C. (1974) *Nature (London) 248*, 338–339.
Cozzone, P. J., Nelson, D. J., & Jardetsky, O. (1974) *Biochem. Biophys. Res. Commun. 60*, 341–347.
Curmi, P. M. G., Barden, J. A., & dos Remedios, C. G. (1982) *Eur. J. Biochem. 122*, 239–244.
De Marco, A., Llinas, M., & Wüthrich, K. (1978) *Biopolymers 17*, 617–636.
dos Remedios, C. G., & Cooke, R. (1984) *Biochim. Biophys. Acta 788*, 193–205.
Grathwohl, C., & Wüthrich, K. (1976a) *Biopolymers 15*, 2025–2042.
Grathwohl, C., & Wüthrich, K. (1976b) *Biopolymers 15*, 2043–2057.
Hambly, B. D., Barden, J. A., Miki, M., & dos Remedios, C. G. (1986) *BioEssays 4*, 124–128.
Hegyi, G., Szilagyi, L., & Elzinga, M. (1986) *Biochemistry 25*, 5793–5798.
Higashima, T., Kobayashi, J., Nagai, U., & Miyazawa, T. (1979) *Eur. J. Biochem. 97*, 43–57.
Hitchcock-de Gregori, S. E., Mandala, S., & Sachs, G. A. (1982) *J. Biol. Chem. 257*, 12573–12580.
Jardetsky, O., & Roberts, G. C. K. (1981) *NMR in Molecular Biology*, Academic Press, New York.
Johnson, C. E., & Bovey, F. A. (1958) *J. Chem. Phys. 29*, 1012–1014.
Jones, C. R., Sikakana, C. T., Hehir, S., Kuo, M.-C., & Gibbons, W. A. (1978) *Biophys. J. 24*, 815–832.
Kabsch, W., Mannherz, H. G., & Suck, D. (1985) *EMBO J. 4*, 2113–2118.
Kirschner, M. W. (1980) *J. Cell Biol. 86*, 330–334.
Kopple, K. D., Ohnishi, M., & Go, A. (1963) *J. Am. Chem. Soc. 91*, 4264–4272.
Korn, E. D. (1982) *Physiol. Rev. 62*, 672–737.
Kuwayami, H., & Yount, R. G. (1986) *Biophys. J. 49*, 454a.
Levitt, M. (1976) *J. Mol. Biol. 104*, 59–107.
Lu, R. C., & Szilagyi, L. (1981) *Biochemistry 20*, 5914–5919.
Mihashi, K., & Wahl, P. (1975) *FEBS Lett. 52*, 8–12.
Miki, M., & Wahl, P. (1984) *Biochim. Biophys. Acta 786*, 188–196.
Miki, M., Barden, J. A., & dos Remedios, C. G. (1986) *Biochim. Biophys. Acta 872*, 76–82.
Muszbek, L., & Laki, K. (1974) *Proc. Natl. Acad. Sci. U.S.A. 71*, 2208–2211.
Neuhaus, J.-M., Wanger, M., Keiser, T., & Wegner, A. (1983) *J. Muscle Res. Cell Motil. 4*, 507–527.
Nozaki, Y., & Tanford, C. (1971) *J. Biol. Chem. 246*, 2211–2217.
Pardee, J. D., & Spudich, J. A. (1982) *J. Cell Biol. 93*, 648–654.

Pollard, T. D., & Weeds, A. G. (1984) *FEBS Lett. 170*, 94–98.
Schulz, G. E., & Schirmer, R. H. (1979) *Principles of Protein Structure*, Springer-Verlag, New York.
Tanswell, P., Thornton, J. M., Korda, A. V., & Williams, R. J. P. (1975) *Eur. J. Biochem. 57*, 135–145.
Vandekerckhove, J., Deboben, A., Nassal, M., & Wieland, T. (1985) *EMBO J. 4*, 2815–2818.
Waechter, F., & Engel, J. (1977) *Eur. J. Biochem. 74*, 227–232.
Walker, J. E., Saraste, M., Runswick, M. J., & Gay, N. J. (1982) *EMBO J. 1*, 945–951.
Wanger, M., Keiser, T., Neuhaus, J.-M., & Wegner, A. (1985) *Can. J. Biochem. Cell Biol. 63*, 414–421.
Wegner, A. (1976) *J. Mol. Biol. 108*, 139–150.

Structure–Activity Relationships in Engineered Proteins: Analysis of Use of Binding Energy by Linear Free Energy Relationships†

Alan R. Fersht,* Robin J. Leatherbarrow, and Tim N. C. Wells
Department of Chemistry, Imperial College of Science and Technology, London SW7 2AY, U.K.
Received January 21, 1987; Revised Manuscript Received April 27, 1987

ABSTRACT: The activity of mutant enzymes can be analyzed quantitatively by structure–activity relationships in a manner analogous to Brønsted or Hammett plots for simple organic reactions. The slopes of such plots, the β values, indicate for the enzymatic reactions the fraction of the overall binding energy used in stabilizing particular complexes. In particular, information can be derived about the interactions between the enzyme and the transition state. The activities of many mutant tyrosyl-tRNA synthetases fit well simple linear free energy relationships. The formation of enzyme-bound tyrosyl adenylate (E·Tyr-AMP) from enzyme-bound tyrosine and ATP (E·Tyr·ATP) results in an increase in binding energy between the enzyme and the side chain of tyrosine and the ribose ring of ATP. Linear free energy plots of enzymes mutated in these positions give the fraction of the binding energy change that occurs on formation of the transition state for the chemical reaction and the various complexes. It is shown that groups that specifically stabilize the transition state of the reaction are characterized by β values $\gg 1$. This is found for residues that bind the γ-phosphate of ATP (Thr-40 and His-45) and have previously been postulated to be involved in transition-state stabilization. The importance of linear free energy plots is that (i) they bring order to the analysis of structure–activity relationships since they allow a large amount of data to be simplified and systematized, (ii) they allow transition-state structure to be inferred from ground-state structure, and (iii), perhaps the most important point at this stage of our knowledge in understanding enzyme structure, they collectively show trends, and exceptions are readily apparent. The observation that the activities of a large number of mutants of the tyrosyl-tRNA synthetase conform to linear free energy equations is the best evidence yet that mutation of the enzyme is probing general properties and trends in the relationship between structure and activity.

The quintessential feature of enzyme catalysis is the use of binding energy to give rate enhancement. It may be shown quite simply by theory (see Appendix) that the increase in rate between an enzyme-catalyzed reaction and its uncatalyzed counterpart in aqueous solution proceeding by the same transition states and intermediates is directly related to the dissociation constants of the substrates, transition states, intermediates, and products from the enzyme. The free energy of transfer of the reagents from water to enzyme is responsible for lowering the free energy of activation and for altering equilibrium constants between enzyme-bound reagents. Thus, to understand enzyme catalysis, one must determine the interaction energies between the enzyme and reagents throughout the complete reaction profile and the energetic changes within the enzyme itself.

Site-directed mutagenesis is eminently suited to studying such structure–activity relationships since the structure of an enzyme may be systematically varied. Unfortunately, protein engineering is an invasive technique since mutagenesis perturbs the very system it studies. The structures of mutant enzymes may be studied by X-ray crystallography or spectroscopy, which may detect changes in structure. But, these techniques can be applied only to stable complexes and cannot be used for examining the important structure for determination of rate, the transition state. Further, X-ray crystallography may not have sufficient resolution for detecting miniscule changes in the structure of an enzyme or its solvation shell that cause significant changes in energetics of catalysis. The only means at present of probing transition-state structure experimentally is the use of kinetics. Accordingly, we are attempting to devise kinetic methods that may be applied in conjunction with X-ray crystallographic data to analyze structure–activity relationships of enzymes and, in particular, how binding energy is utilized. In this paper, we outline the theory of how the use of binding energy may be analyzed by protein engineering, propose criteria for the design of experiments that are open to interpretation by such theory, and apply the theory to reactions of a particular set of mutants of the tyrosyl-tRNA synthetase from *Bacillus stearothermophilus*.

Application of Linear Free Energy Relationships. A traditional way of probing transition-state structure in the reactions of simple organic molecules is the construction of linear

† This work was funded by the Medical Research Council of the U.K.

0006-2960/87/0426-6030$01.50/0